

Thermal induced transformations in glassy chalcogenides $\text{Si}_x\text{Te}_{60-x}\text{As}_{30}\text{Ge}_{10}$

M. H. EL-FOULY, A. F. MAGED, H. H. AMER

National Centre for Radiation Research and Technology, Nasr City, Cairo, Egypt

M. A. MORSEY

Physics Department, Faculty of Science, Cairo University, Beni Suef, Egypt

Temperature-induced transformations are considered to be interesting characteristic properties of amorphous materials including the $\text{Si}_x\text{Te}_{60-x}\text{As}_{30}\text{Ge}_{10}$ system, with $x = 5, 10, 12$ and 20 . Density (ρ), X-ray diffraction and differential thermal analysis (DTA) were used to characterize the compositions. DTA traces of each glass composition at different heating rates from 5 to $30^\circ\text{C min}^{-1}$ were obtained and interpreted. Fast and slow cooling cycles were used to determine the rate of structure formation. Cycling studies of materials show no memory effect but only ovonic switching action. The compositional dependence of the crystallization activation energy (E) and the coefficient of glass-forming tendency (K_{gl}) have been calculated. The thermal transition temperatures and associated changes in specific heat have been examined as a function of the Te/Si ratio by differential scanning calorimetry. It was found that ρ and E increase linearly with increasing tellurium content, while the heat capacity (c_p) and K_{gl} decrease with increasing tellurium content. $E = 1.54\text{ eV}$ and $c_p = 0.246\text{ J g}^{-1}\text{ K}^{-1}$ for $x = 20$ while $E = 2.74\text{ eV}$ and $c_p = 0.22\text{ J g}^{-1}\text{ K}^{-1}$ for $x = 5$.

1. Introduction

The characteristics of threshold switches have been widely investigated since the original publication by Ovshinsky in 1968 [1] and general surveys of the significant results have been provided recently by Adler *et al.* [2] and Homma *et al.* [3]. The study of crystallization kinetics and the thermal properties of the material of the threshold switches provides a potentially sensitive measure of the differences in the structure.

For the present work, four bulk glassy compositions of the system $\text{Si}_x\text{Te}_{60-x}\text{As}_{30}\text{Ge}_{10}$ ($x = 5, 10, 12$ and 20) were prepared by heating mixtures of the elements (99.999% purity) in vacuum ($\approx 10^{-6}$ torr) sealed fused silica ampoules at 800°C for 8 h in which the molten solution was occasionally shaken vigorously, then followed by liquid nitrogen quenching, yielding a high cooling rate [4, 5]. Details of the experimental arrangement and measuring techniques for the differential thermal analysis (DTA), differential scanning calorimetry (DSC) (Shimadzu model DT30 and DS30), hydrostatic density and X-ray (CoK α source) are the same as those described elsewhere [6].

2. Results and discussion

The density of the prepared amorphous glasses of the system $\text{Si}_x\text{Te}_{60-x}\text{As}_{30}\text{Ge}_{10}$ was determined by the hydrostatic method [7] with an accuracy of $\pm 0.05\%$. Fig. 1 shows the variation of density, ρ , with tellurium content. The value of ρ increases linearly from 4.90 to 5.79 g cm^{-3} with increasing tellurium content indicat-

ing the additive nature of density as a character of the glassy structure.

X-ray diffraction patterns of crushed samples of $\text{Si}_x\text{Te}_{60-x}\text{As}_{30}\text{Ge}_{10}$ show no characteristic diffraction lines, indicating the absence of crystalline structure. However, a short-range ordering characterizes the amorphous phase. The diffraction pattern in Fig. 2 is similar to that of $\text{As}_2\text{Se}_3\text{-As}_2\text{S}_3$ [8] and $\text{As}_2\text{Se}_3\text{-As}_2\text{Te}_3$ [9]. The pattern has two stepped humps around

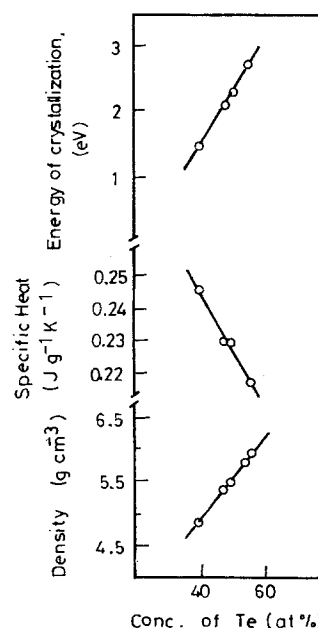


Figure 1 Dependence of density, specific heat and energy of crystallization on tellurium content of the system $\text{Si}_x\text{Te}_{60-x}\text{As}_{30}\text{Ge}_{10}$.

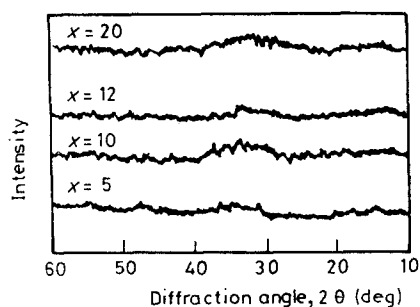


Figure 2 X-ray diffraction patterns of the bulk samples of the system $\text{Si}_x\text{Te}_{60-x}\text{As}_{30}\text{Ge}_{10}$.

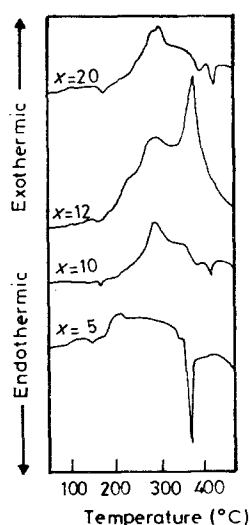


Figure 3 DTA thermograms for the system $\text{Si}_x\text{Te}_{60-x}\text{As}_{30}\text{Ge}_{10}$ at $\phi = 10^\circ\text{C min}^{-1}$.

the Bragg angles 12° to 19° and 20° to 40° ($2\theta^\circ$), respectively. The second has the highest intensity and occupies the largest angular range. This means that the second possesses the highest contribution of diffracting atomic planes.

The characteristic difference between a structurally stable material and a reversible material is demonstrated most simply by DTA [10]. A number of typical DTA scans at a rate of $10^\circ\text{C min}^{-1}$ are shown in Fig. 3 for the four glasses under investigation. All the thermograms are characterized by the presence of an endothermic effect of softening at $T = T_g$, occurring over a temperature range of 165 to 185°C . The value of T_g decreases with increasing tellurium concentration. This may indicate a tendency for weaker bonding in tellurium-rich glasses. Also from Fig. 3 it can be seen that the crystallization peak (T_c) decreases with increasing Te/Si ratio at constant heating rate with the

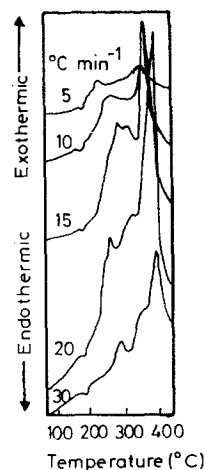


Figure 4 DTA thermograms of the composition $\text{Si}_{12}\text{Te}_{48}\text{As}_{30}\text{Ge}_{10}$ at different rates.

exception of composition $x = 12$. Following the crystallization exothermic peaks, the endothermic peaks due to melting of crystalline material appear on the DTA traces in Fig. 3. The melting temperature (T_m) of composition $x = 12$ does not appear on its DTA trace; it may appear at higher temperature. For compositions $x = 10, 20$, two melting peaks appear on the DTA traces, but due to the broadening of the crystallization peaks and their shifting towards the higher temperature region, the first melting peak is overlapped by part of the crystallization peak. The value of T_m increases with increasing silicon content. Table I gives the observed transition temperatures at a rate of $10^\circ\text{C min}^{-1}$ and the coefficients of glass forming tendency, K_{gl} [11, 12], which are small and increase with increasing silicon content.

DTA traces in Fig. 4 for the composition $\text{Si}_{12}\text{Te}_{48}\text{As}_{30}\text{Ge}_{10}$ show the kinetic crystallization temperature, T_c , which follows T_g at different heating rates. T_c is dependent on the heating rate because crystallization is a kinetic, rather than an equilibrium thermodynamic process for the glasses. At low heating rates ($5, 10, 15^\circ\text{C min}^{-1}$) the DTA traces show two crystallization peaks, which at higher heating rates ($20, 30^\circ\text{C min}^{-1}$) more peaks appear.

The effect of heating rate, ϕ , on the DTA traces of compounds $x = 5, 10$ and 20 was also investigated and it is identical to compound $x = 12$. It was also found that when ϕ increases, the areas under the crystallization and melting peaks of the DTA traces of the system $\text{Si}_x\text{Te}_{60-x}\text{As}_{30}\text{Ge}_{10}$ increase, with some exceptions. The question arises as to why the areas under the crystallization and melting peaks are smaller at low heating rate (i.e. only a small amount of

TABLE I The density and DTA data of the investigated glasses in the system $\text{Si}_x\text{Te}_{60-x}\text{As}_{30}\text{Ge}_{10}$ ($\phi = 10^\circ\text{C min}^{-1}$) as a function of composition. The tendency to form the glass is calculated according to the formula $K_{gl} = (T_c - T_g)/(T_m - T_c)$, using the temperatures in K [11]

Composition	Density (g cm^{-3})	T_g ($^\circ\text{C}$)	T_{c1} ($^\circ\text{C}$)		T_{c2} ($^\circ\text{C}$)		T_m ($^\circ\text{C}$)		K_{gl}
			Begin	Peak	Begin	Peak	Begin	Peak	
$\text{Si}_{20}\text{Te}_{40}\text{As}_{30}\text{Ge}_{10}$	4.90	185	200	295	—	—	395	408	0.97
$\text{Si}_{12}\text{Te}_{48}\text{As}_{30}\text{Ge}_{10}$	5.41	178	230	290	340	365	—	—	—
$\text{Si}_{10}\text{Te}_{50}\text{As}_{30}\text{Ge}_{10}$	5.47	172	240	285	325	388	395	405	0.94
$\text{Si}_5\text{Te}_{55}\text{As}_{30}\text{Ge}_{10}$	5.79	165	175	202	—	—	345	360	0.23

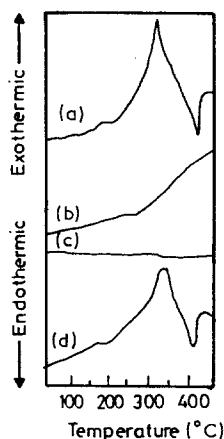


Figure 5 DTA thermograms of $\text{Si}_{10}\text{Te}_{50}\text{As}_{30}\text{Ge}_{10}$: (a) heating curve at $30^\circ\text{C min}^{-1}$, (b) fast cooling at $50^\circ\text{C min}^{-1}$, (c) slow cooling at 5°C min^{-1} , and (d) heating again at $30^\circ\text{C min}^{-1}$.

the sample material has been crystallized) and may be enlarged at higher heating rates. Turnbull [13] has pointed out that the resistance of liquid and glasses to nucleation implies something about their structure. If an amorphous material contained microcrystalline regions, there would be no nucleation barrier, and the crystallization kinetics would be limited only by growth. Thus, at temperatures below the melting point, slow crystallization kinetics would indicate that nucleation was required.

The heat capacity at constant pressure, c_p , has been determined for all glasses under investigation in the system $\text{Si}_x\text{Te}_{60-x}\text{As}_{30}\text{Ge}_{10}$ by using differential scanning calorimetry measurements. The data were taken over the temperature range from room temperature to 200°C .

Fig. 1 shows the compositional dependence of the slope of the linear plots of $c_p = f(T)$. This figure indicates that the value of c_p ($\text{J g}^{-1}\text{K}^{-1}$) slightly increases linearly with increasing silicon concentration. Also, the values of specific heat of each composition are nearly constant over the temperature range 70 to 140°C . The DTA thermograms of heating and cooling cycles are obtained for $x = 10$ and are shown in Fig. 5. This figure shows that the fast rate of cooling (b) and the slow rate of cooling (c) do not exhibit any reaction.

The activation energy of crystallization (E) can be calculated from the shifts in the T_p (the maximum of T_c) values with the heating rate, ϕ [14] by

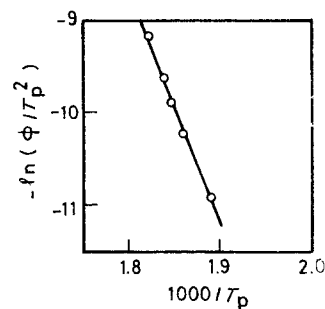


Figure 6 Plot of $\ln(\phi/T_p^2)$ against $1/T_p$ according to the Kissinger method for glassy $\text{Si}_{12}\text{Te}_{48}\text{As}_{30}\text{Ge}_{10}$ for the first peak.

$$\frac{d \ln(\phi/T_p^2)}{d(1/T_p)} = \frac{-E}{R}$$

where R is the gas constant. A plot of $\ln(\phi/T_p^2)$ against T_p^{-1} (K^{-1}) is shown in Fig. 6 for the composition $x = 12$. A straight line could be fitted to give an activation energy for the first peak. Table II gives the values of activation energy of crystallization (E) for the glasses under investigation. Fig. 1 shows that the crystallization activation energy increases linearly with increasing tellurium content.

References

1. S. R. OVSHINSKY, *Phys. Rev. Lett.* **21** (1968) 1450.
2. D. ADLER, H. K. HENISCH and S. N. MOTT, *Rev. Mod. Phys.* **50** (1978) 209.
3. K. HOMMA, H. K. HENISCH and S. R. OVSHINSKY, *J. Non-Cryst. Solids* **35, 36** (1980) 1105.
4. D. R. UHLMAN, *ibid.* **25** (1977) 44.
5. C. BERGMAN, I. AVROMOV, C. Y. ZAHRA and J. C. MATHIEU, *ibid.* **70** (1985) 367.
6. M. F. KOTKATA, M. H. EL-FOULY and M. A. MORSY, *J. Thermal Anal.* **32** (1987) 417.
7. R. L. MYULLER, "Khimia Tverdovo Tela" (Leningrad State University, Leningrad 1965) Ch. 9.
8. E. S. RONALD, *J. Non-Cryst. Solids* **8-10** (1972) 598.
9. S. A. SALEH, M. F. KOTKATA and M. K. ELMOUSLY, *Proc. Math. Phys. Soc. Egypt* **42** (1976) 83.
10. H. FRITZSCHE and R. O. OVSHINSKY, *J. Non-Cryst. Solids* **2** (1970) 148.
11. A. HRUBY, *Czech. J. Phys. B* **22** (1972) 1187.
12. L. CERVINKA and A. HRUBY, *J. Non-Cryst. Solids* **34** (1979) 275.
13. D. TURNBULL, *J. Phys. Chem.* **66** (1962) 609.
14. H. E. KISSINGER, *Anal. Chem.* **29** (1957) 1702.

Received 21 November 1988
and accepted 24 August 1989

TABLE II Activation energy and specific heat for the vitreous-crystalline temperature of the composition of $\text{Si}_x\text{Te}_{60-x}\text{As}_{30}\text{Ge}_{10}$

Composition	Activation energy of crystal, E (eV)		Specific heat, c_p ($\text{J g}^{-1}\text{K}^{-1}$) from 70 to 140°C
	First peak	Second peak	
$\text{Si}_{20}\text{Te}_{40}\text{As}_{30}\text{Ge}_{10}$	1.54	—	0.246
$\text{Si}_{12}\text{Te}_{48}\text{As}_{30}\text{Ge}_{10}$	2.05	2.40	0.23
$\text{Si}_{10}\text{Te}_{50}\text{As}_{30}\text{Ge}_{10}$	2.31	2.57	0.23
$\text{Si}_5\text{Te}_{55}\text{As}_{30}\text{Ge}_{10}$	2.74	—	0.22